

Solution for the elastic field in a layered medium under axisymmetric contact loading

C Fretigny and A Chateauinois

Laboratoire de Physico-Chimie des Polymères et des Milieux Dispersés, UPMC, CNRS UMR 7615, Ecole Supérieure de Physique et Chimie Industrielles (ESPCI), 10, rue Vauquelin, 75231 Paris Cedex 05, France

E-mail: antoine.chateauinois@espci.fr

Received 4 April 2007, in final form 9 July 2007

Published 30 August 2007

Online at stacks.iop.org/JPhysD/40/5418

Abstract

This study addresses the problem of the calculation of the elastic stress and displacement field within isotropic layered media in frictionless contact with rigid axisymmetric indenters. For a prescribed surface stress distribution, the integral transform approach is recalled using a matrix formulation which lends itself to generalizations to multilayered systems. It leads to an analytical solution for the Hankel transform of the elastic field which can readily be numerically inverted in the real space using available discrete Hankel transform algorithms. As an example, the shear stresses induced by the sphere indentation of a coated substrate are calculated as a function of the geometrical confinement of the contact and of the compressibility of the layer. The calculation was carried out using the surface pressure distribution provided by an exact solution to the coated contact problem. In addition, the elastic fields were also determined using an elliptic approximation of the contact pressure distribution. It is shown that the interface shear stress is strongly dependent on the details of the applied pressure profile close to the edge of the contact. In confined layers close to incompressibility, the elliptic approximation is found to result in a systematic overestimate of the interface shear stresses.

1. Introduction

The contact problem of layered isotropic elastic solids is of considerable interest in many areas of physics and solid mechanics. Typical applications include tribological coatings, magnetic data storage and layered composites. In all these applications, a knowledge of the stress fields generated within the film and at the interface is often required to predict the performance and reliability of the coated systems. Of particular importance is the determination of the shear stress distribution at the interface where delamination processes are often observed. From an historical perspective, the theoretical analysis of elastic layered contacts was initially based on integral transforms methods. Starting from the basic equation of elasticity and writing the boundary conditions at the interface between the layers, analytical expressions for the Fourier or Hankel transforms of displacements and stresses

can be obtained for a prescribed distribution of the surface stresses. The theoretical basis of this approach can be found in a paper by Bufler [1], where formal expressions for the stress and displacements fields are derived in the Fourier space in the case of complete adhesion or no adhesion between the layers. Early developments following these lines include the works of Burmister [2–4], Harding and Sneddon [5], Barovich *et al* [6], Chen [7] and Gupta and Walowit [8]. In all these studies, specific solutions for the elastic field are established for normal contact situations differing in the surface pressure distribution, in the number of layers and in the two- or three-dimensional nature of the problem. The integral transform approach was also applied to the problem of the contact stresses generated by Coulomb's friction (e.g. [6, 9–11]). More recently, it was also extended to adhesive contacts on layered substrates within the framework of either the Johnson–Kendall–Roberts (JKR) [12, 13] or Maugis–Dugdale (MD) [14] theories.

The integral transforms involved in these calculations were initially evaluated using conventional numerical integration methods. However, some obstacles were encountered during this computation stage. As pointed out by Chen [7], the integrals become rather slowly convergent at the surface of the top layer near the boundary of the loaded region. This difficulty is especially acute when the ratio of the layer thickness to the contact width (or radius) becomes small. As a consequence, calculations where the coating is highly confined within the contact were systematically discarded despite their practical importance in many tribological situations. These computational limitations were, at least partly, circumvented by using discrete transforms instead of integral ones [15–18].

A common feature of all the above-mentioned models is that the stress and displacement fields are calculated for a prescribed load distribution acting on the surface of the layered substrate, which has to be obtained from a preliminary resolution of the contact problem. However, the latter is a mixed boundary value problem, where the surface stresses are usually specified outside the contact area and the surface displacement within the contact. The theoretical resolution of this mixed boundary problem in layered contacts has long been a source of major complications. In the absence of any explicit closed-form solution, some early calculations of the elastic field within the layers simply assume an arbitrary semi-elliptical or uniform distribution of the surface normal stress (e.g. in [6, 7, 19]). More refined approaches involve approximate numerical solutions to the contact problem. Following an idea initially introduced by Bentall and Johnson [20], the unknown pressure distribution is represented as a linear combination of a suitable set of basis functions whose Fourier or Hankel transforms are known analytically [8–10, 21, 22]. This set of basis functions is assembled to represent the contact pressure distribution so that the displacement within the contact area approximates the real displacement boundary conditions in accordance with some arbitrary residual error criterion. At the cost of an increased complexity in the set of basis functions, this approach has been extended to the calculation of the contact pressure induced by non-axisymmetric rigid indenters including parabolic, quadrilateral and triangular punches [7, 23, 24]. In addition, the efficiency of these calculations was greatly improved by the use of iterative FFT calculations [15, 18, 25].

Alternatively, asymptotic solutions to the contact problem were also derived for limit cases such as the sphere and cone indentation of a confined elastic layer lying on a rigid substrate [26]. Another approximate approach by Yoffe [27] focuses on the calculation of an additional stress field which would compensate the inhomogeneity of the layered solid during its indentation by a rigid flat punch. Using a method introduced by Fabrikant [28], Schwartz [29] also solved the contact problem from an electrostatic like method of image, leading to the calculation of the sum of an infinite series.

However, these complexities in the resolution of the contact problem can be avoided by using some exact quasi-analytical solutions to the frictionless contact problem of a coated substrate with axisymmetric indenters [30, 31]. If some appropriate auxiliary functions are introduced in the formulation of the contact equations, it can be shown that the mixed boundary conditions contact problem can be inverted in

the real space in the form of a single integral equation. The latter can readily be solved numerically in order to provide the distribution of the surface normal stress. Then, it is possible to obtain the elastic field in the material from these exact solutions. In this paper, the integral transform formalism is briefly recalled. As an application of this approach, the distribution of the shear stress at the film/substrate interface will be discussed for different levels of geometrical confinement of the contact. It is shown that, when the contact size is comparable to the film thickness, the use of a precise contact pressure distribution is necessary to describe interfacial stresses which may be responsible for delamination of the layer under indentation.

2. Formulation of the model

As mentioned in the introduction section, stresses and displacements at the surface of an elastically isotropic layered medium under the action of surface displacements or stresses have been often calculated. In this section, a short summary of the usually employed methods is given. It is presented using a matrix formulation of the equations [1] as it may be easier to read and it lends itself to generalizations to multilayered systems and to adhesive contacts. Moreover, modern programming languages usually handle numerical matrix computations, which may render the formula easy to use. Explicit expressions of the matrices are given in appendix A. The example of perfect adhesion between the layer and the substrate is detailed. The aim is to introduce a practical formalism for calculating the stress and displacements in the material when a contact is established with a rigid axisymmetric punch, assuming zero friction in the contact area.

2.1. Harding–Sneddon formalism

It has earlier been recognized [5] that, under cylindrical symmetry conditions (along z axis), an auxiliary function $G(\xi, z)$ can be used to express the mechanical fields in an homogeneous linear elastic isotropic medium (shear modulus, μ , Young's modulus, $E = 2\mu(1 + \nu)$, Poisson's ratio, ν). Indeed, Hankel transforms of stress and displacements can be expressed as a linear combination of Hankel transforms of $G(\xi, z)$ and of its three first z -derivative. One can represent these parameters using the vector

$$\Gamma(\xi, z) = [\xi^3 G(\xi, z), \xi^2 G'(\xi, z), \xi G''(\xi, z), G'''(\xi, z)]^\top, \quad (1)$$

where prime symbols stand for z -derivatives. Then, defining, a 'state vector' with four components

$$\Omega(\xi, z) = [\sigma_{zz}|_0(\xi, z), \sigma_{rz}|_1(\xi, z), \xi w|_0(\xi, z), \xi u|_1(\xi, z)]^\top \quad (2)$$

one can express the elastic fields as

$$\Omega(\xi, z) = M\Gamma(\xi, z), \quad (3)$$

where M is a 4×4 matrix detailed in appendix A, which only depends on the mechanical properties of the elastic medium. u and w denote the radial and

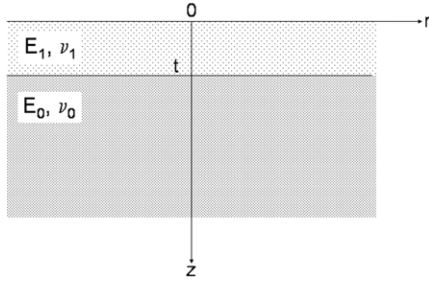


Figure 1. Schematic of the coated contact. E_i and ν_i denote Young's modulus and Poisson's ratio, respectively, of the layer ($i = 1$) and the substrate ($i = 0$).

vertical displacements, respectively. The last two non-zero components of the stress tensor are obtained from the relation

$$[\sigma_{\theta\theta}|_0(\xi, z) + \sigma_{rr}|_0(\xi, z), r\sigma_{\theta\theta}|_1(\xi, z) - r\sigma_{rr}|_1(\xi, z)]^\top = N\Gamma(\xi, z) \quad (4)$$

(N is a 2×4 matrix detailed in [appendix A](#)). In these expressions the notation

$$\varphi|_q(\xi, z) = \int_0^\infty \varphi(r, z) J_q(\xi r) r dr \quad (5)$$

stands for the order q Hankel transform of the function $\varphi(r, z)$ ($J_q(x)$ is the Bessel function of order q).

As $G(\xi, z)$ obeys the differential equation

$$\left(\frac{\partial^2}{\partial z^2} - \xi^2 \right)^2 G(\xi, z) = 0, \quad (6)$$

it can be explicitly written in the form

$$G(\xi, z) = [A(\xi) + \xi z B(\xi)] \exp(-\xi z) + [C(\xi) + \xi z D(\xi)] \exp(\xi z), \quad (7)$$

where $A(\xi)$, $B(\xi)$, $C(\xi)$, $D(\xi)$ are some functions of ξ .

The first order differential equation for the vector $\Gamma(\xi, z)$ corresponding to (6) can be written as

$$\frac{\partial}{\partial z} \Gamma(\xi, z) = \xi P \Gamma(\xi, z), \quad (8)$$

which solution is

$$\Gamma(\xi, z') = \Pi[\xi(z' - z)] \Gamma(\xi, z), \quad (9)$$

where

$$\Pi(s) = \exp[sP], \quad (10)$$

where P is a 4×4 matrix given in [appendix A](#). Then, propagation of the Hankel transforms of the mechanical fields from one plane to another is easily described using this propagator.

2.2. Coated substrate

Consider now an isotropic elastic layer (thickness t , Young modulus E_1 , Poisson ratio ν_1) on top of an isotropic elastic semi-infinite substrate (Young modulus E_0 , Poisson ratio ν_0). Origin of z axis is taken at the surface (figure 1). Auxiliary functions $G_0(\xi, z)$ and $G_1(\xi, z)$ (and their corresponding

vectors $\Gamma_0(\xi, z)$ and $\Gamma_1(\xi, z)$) as well as matrices M_0 and M_1 can be defined in the substrate and in the layer, respectively. Boundary conditions at the interface are expressed using displacements and stress in both regions. In the case of a perfect adhesion at the interface, continuity of the stress components σ_{zz} and σ_{rz} and of the z and r displacements (w and u , respectively) must be expressed. A 'state vector' can be defined in the medium p ($p = 0, 1$) as

$$\Omega_p(\xi, z) = [\sigma_{zz}|_p(\xi, z), \sigma_{rz}|_p(\xi, z), \xi w|_p(\xi, z), \xi u|_p(\xi, z)]^\top. \quad (11)$$

When a perfect adhesion exists at the interface, boundary conditions at the interface are expressed through the equation

$$\Omega_1(\xi, t) = \Omega_0(\xi, t), \quad (12)$$

which represents the continuity of the displacements and stress. This relation can be written as

$$M_1 \Gamma_1(\xi, t) = M_0 \Gamma_0(\xi, t). \quad (13)$$

Finally, the state vector on the surface $\Omega_1(\xi, 0) = M_1 \Gamma_1(\xi, 0)$ is connected to the vector $\Gamma_0(\xi, t)$ through the propagation relation (9) and boundary condition (13):

$$\Omega_1(\xi, 0) = M_1 \Pi[-\xi t] M_1^{-1} M_0 \Gamma_0(\xi, t). \quad (14)$$

Recalling the general form for $G_0(\xi, z)$ given in (7):

$$G_0(\xi, z) = [A_0(\xi) + \xi z B_0(\xi)] \exp(-\xi z) + [C_0(\xi) + \xi z D_0(\xi)] \exp(\xi z), \quad (15)$$

there exists a 4×4 matrix $\Theta(\xi z)$ such that

$$\Gamma_0(\xi, z) = \xi^3 \Theta(\xi z) V_0(\xi, z), \quad (16)$$

$$V_0(\xi, z) = [A_0(\xi) \exp(-\xi z), B_0(\xi) \exp(-\xi z),$$

$$C_0(\xi) \exp(\xi z), D_0(\xi) \exp(\xi z)]^\top. \quad (17)$$

Therefore, (14) can be inverted as

$$\xi^{-3} F \Omega_1(\xi, 0) = V_0(\xi, t) \quad (18)$$

with

$$F = \Theta^{-1}(\xi t) M_0^{-1} M_1 \Pi[\xi t] M_1^{-1}.$$

In the substrate, non-divergence of the field for an infinite depth imposes that the solution of the differential equation (6) is such that $C_0(\xi) = D_0(\xi) = 0$. Thus, (18) can be written as

$$\xi^{-3} \exp(\xi t) F \Omega_1(\xi, 0) = [A_0(\xi), B_0(\xi), 0, 0]^\top. \quad (19)$$

Considering that the last two components of the vector in the rhs of (19) are zero, two linear equations mixing $\sigma_{zz}|_0(\xi, 0)$, $\sigma_{rz}|_1(\xi, 0)$, $\xi w|_0(\xi, 0)$ and $\xi u|_1(\xi, 0)$ can be deduced:

$$\Phi \Omega_1(\xi, 0) = [0, 0]^\top, \quad (20)$$

where Φ is the 2×4 sub-matrix obtained from the two lower rows of F .

In a frictionless contact problem, $\sigma_{rz}|_1(\xi, 0) = 0$. Elimination of the radial displacement $u|_1(\xi, 0)$ between the above two equations then leads to the following linear

relation between the two remaining components, $w|_0(\xi, 0)$ and $\sigma_{zz}|_0(\xi, 0)$:

$$w|_0(\xi, 0) = \frac{X(\xi t)}{\xi} \sigma_{zz}|_0(\xi, 0), \quad (21)$$

which was first derived by Burmister [2] and rediscovered later by others [10, 19, 32].

At this point, generalization of the method to a multilayered system is straightforward: several propagations and boundary condition matchings must successively apply. As an example, for a two layer system (thickness t_1 and t_2), the matrix F reads

$$F = \Theta^{-1}[\xi(t_1 + t_2)]M_0^{-1}M_1\Pi[\xi t_1]M_1^{-1}M_2\Pi[\xi t_2]M_2^{-1}, \quad (22)$$

where indices 2 stand for the external layer. One can deduce the matrix Φ as above and find a linear relation between normal displacements and pressure analogous to (21). For a system made of p layers of thickness t_k ($k = 1, \dots, p$) on a semi-infinite substrate,

$$F = \Theta^{-1}[\xi\tau]M_0^{-1}\Lambda_1 \cdots \Lambda_{p-1}\Lambda_p, \quad (23)$$

where $\tau = t_1 + t_2 + \dots + t_p$ and Λ_k the propagator of the state vector for the layer k reads

$$\Lambda_k = M_k\Pi[\xi t_k]M_k^{-1}. \quad (24)$$

2.3. Elastic fields in the material

If a distribution of external stress $\sigma_{zz}(r, 0)$ and $\sigma_{rz}(r, 0)$ is prescribed at the surface, it is possible to deduce the displacement and stress fields in the layered material using the same formalism (note that in a frictionless contact problem, $\sigma_{rz}(r, 0) = 0$). From relation (3) expressed at $z = 0$

$$M_1\Gamma_1(\xi, 0) = \Omega_1(\xi, 0) \quad (25)$$

retaining the two first equations, one can define a 2×4 sub-matrix M'_1 obtained from the first two rows of M_1 :

$$M'_1\Gamma_1(\xi, 0) = [\sigma_{zz}|_0(\xi, 0), \sigma_{rz}|_1(\xi, 0)]^\top. \quad (26)$$

Using the relation (20) under the form

$$\Phi M_1\Gamma_1(\xi, 0) = [0, 0]^\top \quad (27)$$

one can deduce

$$Q\Gamma_1(\xi, 0) = [\sigma_{zz}|_0(\xi, 0), \sigma_{rz}|_1(\xi, 0), 0, 0]^\top, \quad (28)$$

where Q is a 4×4 matrix built from the superposition of the rows of M'_1 and ΦM_1 . Thus

$$\Gamma_1(\xi, 0) = Q^{-1}[\sigma_{zz}|_0(\xi, 0), \sigma_{rz}|_1(\xi, 0), 0, 0]^\top. \quad (29)$$

Hankel transforms of the displacements and stress in the layer can be deduced from their expression in terms of $\Gamma_1(\xi, z)$, using the propagation relation:

$$\Gamma_1(\xi, z) = \Pi[\xi z]Q^{-1}[\sigma_{zz}|_0(\xi, 0), \sigma_{rz}|_1(\xi, 0), 0, 0]^\top. \quad (30)$$

Once this vector is determined, all mechanical fields can be readily deduced. We obtain directly,

$$[\sigma_{zz}|_0(\xi, z), \sigma_{rz}|_1(\xi, z), \xi w|_0(\xi, z), \xi u|_1(\xi, z)]^\top = M_1\Gamma_1(\xi, z), \quad (31)$$

$$[\sigma_{\theta\theta}|_0(\xi, z) + \sigma_{rr}|_0(\xi, z), r\sigma_{\theta\theta}|_1(\xi, z) - r\sigma_{rr}|_1(\xi, z)]^\top = N_1\Gamma_1(\xi, z) \quad \text{for } 0 \leq z \leq t. \quad (32)$$

To get the mechanical fields in the substrate, it is necessary to calculate $\Gamma_0(\xi, z)$ (with $z > t$) which is deduced from $\Gamma_1(\xi, t)$ by taking into account the boundary conditions at the interface:

$$\Gamma_0(\xi, z) = \Pi[\xi(z-t)]M_0^{-1}M_1\Gamma_1(\xi, t) \quad (33)$$

$$= \Pi[\xi(z-t)]M_0^{-1}M_1\Pi[\xi t] \times Q^{-1}[\sigma_{zz}|_0(\xi, 0), \sigma_{rz}|_1(\xi, 0), 0, 0]^\top \quad (34)$$

and thus

$$[\sigma_{zz}|_0(\xi, z), \sigma_{rz}|_1(\xi, z), \xi w|_0(\xi, z), \xi u|_1(\xi, z)]^\top = M_0\Gamma_0(\xi, z), \quad (35)$$

$$[\sigma_{\theta\theta}|_0(\xi, z) + \sigma_{rr}|_0(\xi, z), r\sigma_{\theta\theta}|_1(\xi, z) - r\sigma_{rr}|_1(\xi, z)]^\top = N_1\Gamma_0(\xi, z) \quad \text{for } z \geq t. \quad (36)$$

For a multilayered system, the procedure is similar for the external layer, provided that Φ is determined from F , according to (23). For deeper layers, it is necessary to take into account the boundary conditions as above.

2.4. Contact conditions

Contact imposes mixed boundary conditions at the surface: Normal displacement is prescribed in the contact region while normal pressure is zero out of this zone. None of the Hankel transforms $\sigma_{zz}|_0(\xi, 0)$ nor $w|_0(\xi, 0)$ are directly known. For frictionless contacts on a coated substrate, a method of resolution of (21) with mixed boundary conditions uses auxiliary functions [30, 31]:

$$\theta(s) = \int_0^\infty \xi d\xi w|_0(\xi, 0) \cos \xi s, \quad (37)$$

$$g(s) = \int_0^\infty d\xi \sigma_{zz}|_0(\xi, 0) \cos \xi s. \quad (38)$$

For given axisymmetric indenter shape and contact radius, numerical resolution of an integral equation allows the determination of both functions:

$$\theta(s) = \frac{2}{\pi} \int_0^\infty \int_0^\infty du d\xi X(\xi t)g(u) \cos \xi u \cos \xi s. \quad (39)$$

As the displacement is prescribed within the contact, it can be shown that $\theta(s)$ is known in this region. As a consequence, $g(s)$ can be determined by numerical inversion of (39). This technique also applies to multilayered materials, since equations similar to (21) are obtained in this case. Thus, from a cosine back-transform of $g(s)$, one can deduce the Hankel transform of the normal pressure $\sigma_{zz}|_0(\xi, 0)$. Then, elastic fields in the materials are obtained from (30), (31) and (33). As it is detailed in [12, 13], this approach can also be readily extended to account for adhesive contact situations.

2.5. Inversion of the Hankel transforms

Displacements and stresses in the direct space can be obtained by numerical Hankel inversion using a fast inversion algorithm (see, for example [33]). As in classical FFT techniques, special care is necessary to adjust the different cut-off and the number of points in order to get accurate results. It can be noted in passing that the calculation of the elastic field does not present any particular numerical problem when the layer is incompressible (i.e. $\nu_1 = 0.5$), as opposed to finite element simulations. In addition, the inversion of the Hankel transform can be carried out accurately over a wide range of reduced moduli and a/t ratios, as it will be shown below.

3. Numerical results

As mentioned in the introduction, the calculation of the elastic stress field in coated contacts has often been carried out assuming an elliptical pressure at the boundary [6, 7, 10, 19, 34]. However, some investigations indicate that the contact pressure distribution at the surface of a layered substrate can deviate significantly from such an elliptic profile [8, 23, 35]. The question thus arises to determine whether the elliptical approximation of the contact pressure can result in significant deviations from the calculated actual stress field within the layered substrate. This question has been addressed in some details by Gupta and Walowit [8] for a cylinder contact from a comparison with the stress fields calculated using true pressure profiles. For a moderate geometrical confinement of the layer (i.e. for a ratio of the contact width to the thickness of the layer close to unity), it was concluded by these authors that the stresses calculated using an elliptical approximation do not differ significantly from the actual ones. In this section, we consider further the validity of the elliptical approximation in the case of sphere indentation and for an extended range of contact confinement. For that purpose, the stresses calculated using an elliptical approximation will be compared with that obtained using the actual contact pressure provided by the exact solution to the contact problem [30, 31]. The analysis will focus on the distribution of interface shear stress, which is of importance for the prediction of delamination processes in coated substrates.

In a preliminary step, the exact surface pressure profiles have been determined using the approach derived by Perriot and Barthel [31]. The calculations have been carried out for the case of a soft layer adhesively bounded to a more rigid substrate. The ratio of the reduced Young's modulus of the substrate, E_0^* , to that of the layer, E_1^* , was set between 10 and 100. As an example, a ratio of 50 would correspond to the case of a glass substrate coated with a glassy polymer layer. Changes in Poisson's ratio of the layer have also been considered, from 0.4 to an incompressible case (i.e. $\nu_1 = 0.5$), while Poisson's ratio of the substrate was kept constant and equal to 0.2. The contact calculation has been repeated for several ratios of the contact radius, a , to the film thickness, t which is the input of the model. The corresponding indentation loads are given in appendix B. In order to investigate the validity of the elliptical approximation, the actual pressure profiles were fitted to a power-law expression in the form

$$p(r) = p_0(1 - r^2/a^2)^n. \tag{40}$$

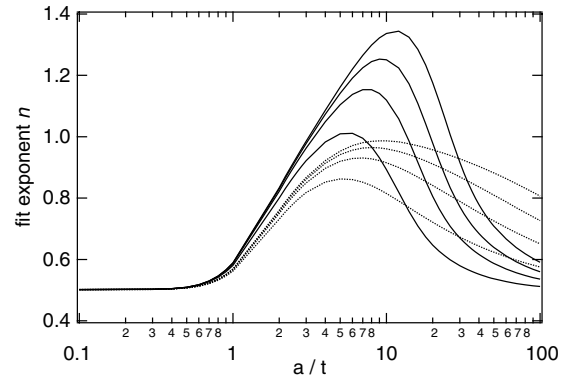


Figure 2. Approximation of the contact pressure distribution by a power-law relation ($p(r) = p_0(1 - r^2/a^2)^n$). The values of the exponent, n , are represented as a function of the ratio of the contact radius to the thickness of the layer. Dotted and solid lines correspond to $\nu_1 = 0.4$ and $\nu_1 = 0.5$, respectively. The ratio of the reduced modulus of the substrate to that of the layer, E_0^*/E_1^* , is, from bottom to top: 10, 25, 50 and 100. ($\nu_0 = 0.2$).

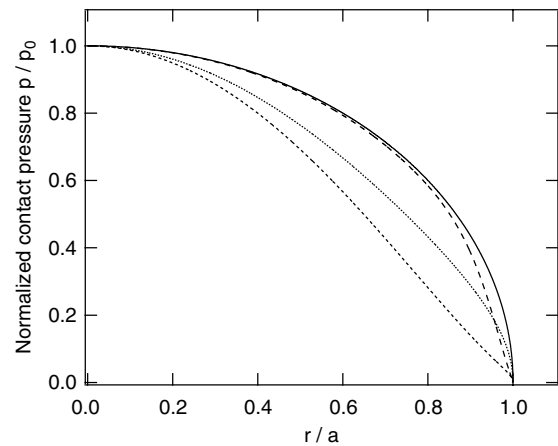


Figure 3. Distribution of the applied contact pressure for different values of the geometrical confinement, a/t , of the contact. The profiles have been normalized with respect to the value, p_0 , of the contact pressure at the centre of the contact ($r = 0$). (.....) $a/t = 2$; (- - -) $a/t = 10$, (- · - ·) $a/t = 100$, (—) elliptic approximation ($E_0^*/E_1^* = 50$, $\nu_0 = 0.2$, $\nu_1 = 0.5$).

In figure 2, the fit exponent, n , is shown as a function of the contact confinement and for different values of the elastic properties of the layer and the substrate. As it is expected, the pressure profile is close to elliptical (i.e. $n = 0.5$) when the confinement is low ($a/t < 1$), i.e. when the contact behaviour is close to the Hertzian response of the layer. Similarly, the profiles tend to an elliptical distribution when a/t is close to 100 as a result of the increased Hertzian contribution of the substrate. On the other hand, it comes out that the contact pressure can differ significantly from the elliptical approximation when the confinement of the layer is varying between these two limit cases. This deviation is enhanced when the ratio of the reduced modulus of the substrate to that of the layer is enhanced. It is also especially marked in the case of an incompressible layer, where exponents greater than 1.3 can be obtained when a/t is close to 10. Further evidence of the non-Hertzian behaviour is also shown in figure 3 which details the shape of some of the calculated pressure profiles in

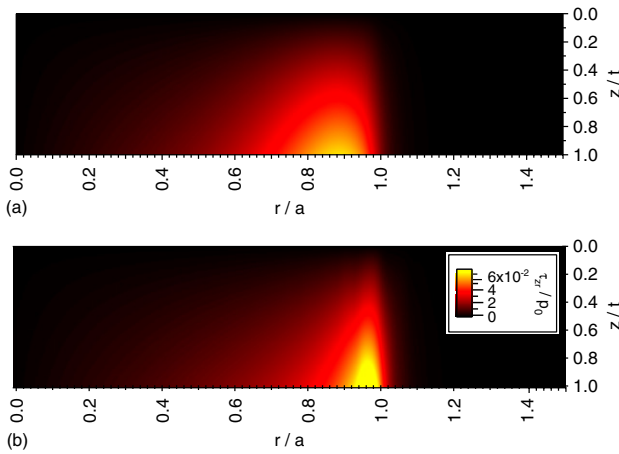


Figure 4. Calculated shear stress distributions within a confined ($a/t = 40$) incompressible ($\nu_1 = 0.5$) layer. (a) calculation using the actual pressure profile; (b) calculation using an elliptic approximation of the contact pressure distribution. The shear stresses have been normalized with respect to the maximum contact pressure, p_0 of the actual pressure profile. In the case of the elliptic approximation, the maximum contact pressure was calculated in order to yield the same contact load as that of the exact solution. $E_0^*/E_1^* = 50$, $\nu_0 = 0.2$.

(This figure is in colour only in the electronic version)

the incompressible case. This preliminary analysis therefore shows that, depending on the geometrical confinement of the contact and on the compressibility of the layer, the contact pressure profiles can differ largely from the elliptic assumption.

The sensitivity of the interface shear stress to the shape of the contact pressure profile has subsequently been considered in the case of an incompressible layer. As an example, the calculation has been carried out for a confinement, $a/t = 40$ and for a ratio of the reduced moduli, $E_0^*/E_1^* = 50$. The maximum pressure corresponding to the elliptic approximation was calculated in order to yield a contact load equal to that determined from the exact contact solution at the same a/t value. Figure 4 shows the corresponding shear stress distributions within the layer. In both cases, the maximum shear stress appears to be localized at the film/substrate interface, close to the periphery of the contact. This description is consistent with the general picture which can be drawn for the squeeze of a confined layer between rigid substrates. In such a situation, it turns out that the stresses at the middle of the contact are of essentially hydrostatic nature, whereas shear stresses develop at the periphery of the contact, where the confinement is reduced [36]. In the case of the elliptic approximation, the calculated shear stresses seem to be higher and more strongly localized at the edge of the contact than for the exact calculation. This is confirmed by an examination of the shear stress profiles at the interface (figure 5(a)). As compared with the actual stress profile, the elliptic approximation results in a much sharper shear stress peak whose magnitude is overestimated by a factor of 1.4 for the considered elastic properties and contact confinement. As detailed in appendix B, this overestimate of the maximum interface shear stress is observed when the a/t ratio exceeds a value of about 10. It is also preserved when the ratio of the reduced modulus of the substrate to that of the layer is varied

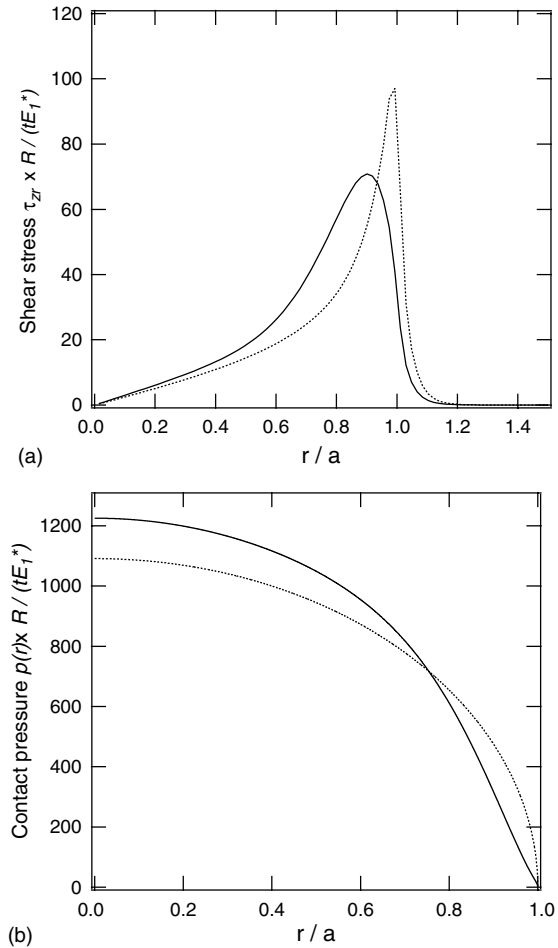


Figure 5. Relation between (a) the interface shear stress in the case of an incompressible layer ($\nu_1 = 0.5$) and (b) the applied contact pressure distribution, for $a/t = 40$. R is the radius of the indenting sphere. (—) exact solution, (·····) elliptic approximation ($E_0^*/E_1^* = 50$, $\nu_0 = 0.2$).

from 10 to 100. From an examination of the corresponding surface pressure profiles (figure 5(b)), it transpires that the sharpness of the shear stress peak close to the edge of the contact is largely driven by the gradient of the applied pressure in this region. The elliptic approximation indeed yield to a much more pronounced contact pressure gradient close to $r = a$. As far as one is interested in the interface shear stress, the theoretical calculations therefore appear to be very sensitive to relatively minor changes in the shape of the pressure profile close to the edge of the contact. An exact contact pressure distribution rather than an approximate solution such as the elliptic profile should therefore be preferred as far as one is concerned with interface shear stresses in layered contacts.

4. Conclusion

A review of the literature is given on the contact problem on a layered medium. The integral transform method for determining the elastic field in a layered medium submitted to an axisymmetric external pressure is presented under a matrix formalism. The case of a single layer on top of a

substrate, with perfect adhesion at the interface, is detailed. When applied to a frictionless contact problem, the result are shown to be sensitive to the accuracy of the pressure profile. By comparison with an exact solution, shearing at the interface is poorly described if an Hertzian pressure profile is assumed. The detailed formalism may be useful to predict delamination properties under indentation situations. It also lends itself to straightforward generalization to a multilayer case. In addition, this approach can readily be applied to adhesive contacts, provided that the surface pressure profile is obtained from a preliminary resolution of the adhesive contact problem using one of the methods introduced in [13, 14]. An example is provided in [13], where the mechanical field in an adhesive layer has been calculated within the assumption of short range adhesive forces.

Acknowledgments

The authors wish to thank Etienne Barthel (CNRS/Saint Gobain, Aubervilliers, France) for many fruitful and stimulating discussions.

Appendix A

$$M = \begin{bmatrix} 0 & -2\mu(2-\nu) & 0 & 2\mu(1-\nu) \\ 2\mu(1-\nu) & 0 & 2\mu\nu & 0 \\ -2(1-\nu) & 0 & 1-2\nu & 0 \\ 0 & 1 & 0 & 0 \end{bmatrix}, \tag{A.1}$$

$$M^{-1} = \begin{bmatrix} 0 & \frac{1-2\nu}{2\mu(1-\nu)} & -\frac{\nu}{1-\nu} & 0 \\ 0 & 0 & 0 & 1 \\ 0 & \frac{1}{\mu} & 1 & 0 \\ \frac{1}{2\mu(1-\nu)} & 0 & 0 & \frac{2-\nu}{1-\nu} \end{bmatrix}, \tag{A.2}$$

$$N = \begin{bmatrix} 0 & 2\mu(1-2\nu) & 0 & 4\mu\nu \\ 0 & 2\mu/\xi & 0 & 0 \end{bmatrix}, \tag{A.3}$$

$$P = \begin{bmatrix} 0 & 1 & 0 & 0 \\ 0 & 0 & 1 & 0 \\ 0 & 0 & 0 & 1 \\ -1 & 0 & 2 & 0 \end{bmatrix}, \tag{A.4}$$

$$\Pi(s) = \frac{1}{2} \begin{bmatrix} 2C - sS & 3S - sC & sS & sC - S \\ S - sC & 2C - sS & S + sC & sS \\ -sS & S - sC & 2C + sS & S + sC \\ -S - sC & -sS & sC + 3S & 2C + sS \end{bmatrix}, \tag{A.5}$$

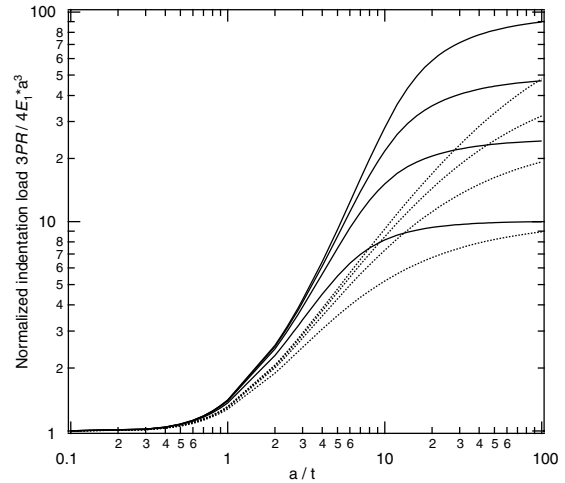


Figure B.1. Non-dimensional indentation load as a function of the ratio of the contact radius to the film thickness. Dotted and solid lines correspond to $\nu_1 = 0.4$ and $\nu_1 = 0.5$, respectively. The ratio of the reduced modulus of the substrate to that of the layer, E_0^*/E_1^* , is, from bottom to top: 10, 25, 50 and 100 ($\nu_0 = 0.2$).

where $S = \sinh(s)$ and $C = \cosh(s)$,

$$\Theta(s) = 4 \begin{bmatrix} 1 & s & 1 & s \\ -1 & -s+1 & 1 & s+1 \\ 1 & s-2 & 1 & s+2 \\ -1 & -s+3 & 1 & s+3 \end{bmatrix}, \tag{A.6}$$

$$\Theta^{-1}(s) = \frac{1}{4} \begin{bmatrix} -s+2 & -3+s & s & -s+1 \\ 1 & -1 & -1 & 1 \\ s+2 & s+3 & -s & -s-1 \\ -1 & -1 & 1 & 1 \end{bmatrix}, \tag{A.7}$$

$$X(s) = \frac{2}{E_1^*} \frac{1 + 4bs \exp(-2s) - ab \exp(-4s)}{1 - (a + b + 4bs^2) \exp(-2s) + ab \exp(-4s)}, \tag{A.8}$$

where

$$a = \frac{\alpha\gamma_0 - \gamma_1}{1 + \alpha\gamma_0}, \quad b = \frac{\alpha - 1}{\alpha + \gamma_1}, \quad \alpha = \frac{\mu_1}{\mu_0}, \tag{A.9}$$

$$\gamma_1 = 3 - 4\nu_1, \quad \gamma_0 = 3 - 4\nu_0, \quad E_1^* = \frac{E_1}{1 - \nu_1^2},$$

$$\Lambda(s) = \frac{1}{1+\gamma} \begin{bmatrix} -2sS + (1+\gamma)C & (1-\gamma)S - 2sC \\ (1-\gamma)S + 2sC & 2sS + (1+\gamma)C \\ (\gamma S - sC)/\mu & -sS/\mu \\ sS/\mu & (\gamma S + sC)/\mu \end{bmatrix} \begin{bmatrix} 4\mu[S - sC] & -4\mu sS \\ 4\mu sS & 4\mu[S + sC] \\ -2sS + (1+\gamma)C & -(1-\gamma)S - 2sC \\ -(1-\gamma)S + 2sC & 2sS + (1+\gamma)C \end{bmatrix}. \tag{A.10}$$

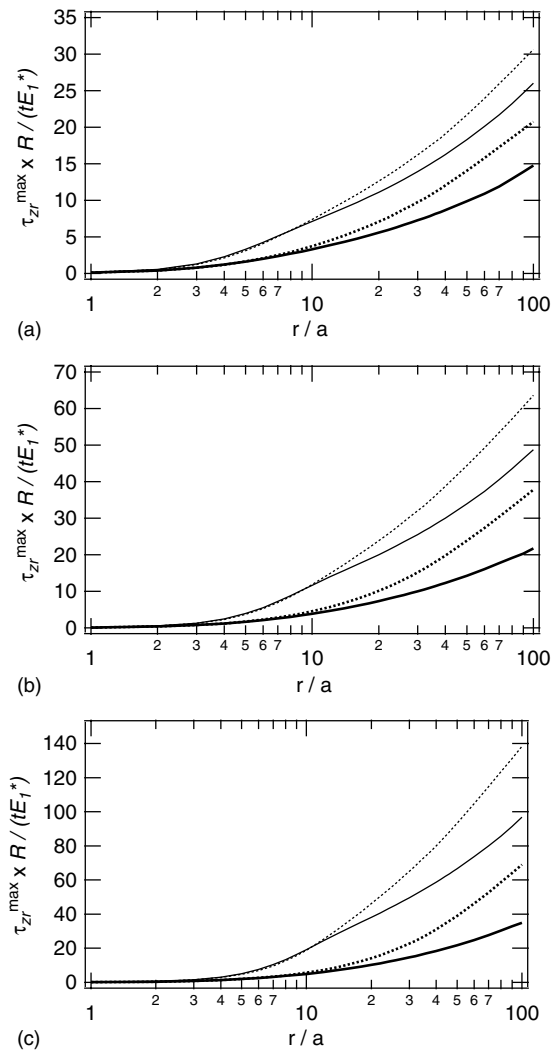


Figure B.2. Maximum shear stress, τ_{zr}^{\max} , at the interface as a function of the geometrical confinement of the contact. Solid and dotted lines correspond to the exact solution and the elliptical approximation, respectively. Thick lines: $\nu_1 = 0.4$; Thin lines: $\nu_1 = 0.5$. R is the radius of the indenting sphere. (a) $E_0^*/E_1^* = 10$; (b) $E_0^*/E_1^* = 50$; (c) $E_0^*/E_1^* = 100$ ($\nu_0 = 0.2$).

Appendix B

All the calculations detailed in the text have been carried out using the geometrical confinement of the contact, a/t , as an input parameter. In order to make useful these results in practical indentation situations, figure B.1 provides the relationship between a/t and the non-dimensional indentation load, $3PR/4E_1^*a^3$.

Figure B.2 give the values of the maximum value of the interface shear stress as a function of the contact confinement and the elastic properties of the layer and the substrate. It can be noted that the elliptic approximation of the surface contact pressure overestimates the actual maximum interface shear stress when the ratio of the contact radius to the film thickness is greater than about 10. The magnitude of this difference between the elliptic approximation and the exact calculation is also enhanced when the ratio E_0^*/E_1^* is increased or when the layer is incompressible (i.e. $\nu_1 = 0.5$).

References

- [1] Buefler H 1971 Theory of elasticity of a multilayered medium *J. Elast.* **1** 125–43
- [2] Burmister D M 1945 The general theory of stresses and displacements in layered systems: I *J. Appl. Phys.* **16** 89–94
- [3] Burmister D M 1945 The general theory of stresses and displacements in layered soil systems: II *J. Appl. Phys.* **16** 126–7
- [4] Burmister D M 1945 The general theory of stresses and displacements in layered soil systems: III *J. Appl. Phys.* **16** 296–302
- [5] Harding J W and Sneddon I N 1945 The elastic stresses produced by the indentation of the plane surface of a semi-infinite elastic solid by a rigid punch *Proc. Camb. Phil. Soc.* **41** 16–26
- [6] Barovich D, Kingsley S C and Ku T C 1964 Stresses on a thin strip or slab with different elastic properties from that of the substrate due to elliptically distributed load *Int. J. Eng. Sci.* **2** 253–68
- [7] Chen W T 1971 Computation of stresses and displacements in a layered elastic medium *Int. J. Eng. Sci.* **9** 775–800
- [8] Gupta P K and Walowit J A 1974 Contact stresses between an elastic cylinder and a layered elastic solid *J. Lubr. Technol.—Trans. ASME* **96** 250–7
- [9] King R B 1987 Sliding contact stresses in a two-dimensional layered elastic half space *Int. J. Solids Struct.* **23** 581–97
- [10] O’Sullivan T C and King R B 1988 Sliding contact stress field due to a spherical indenter on a layered elastic half-space *J. Tribol.—Trans. ASME* **110** 235–40
- [11] Kuo C H and Keer L M 1992 Contact stress analysis of a layered transversely isotropic half-space *J. Tribol.* **114** 253–62
- [12] Barthel E and Perriot A 2007 Adhesive contact to a coated elastic substrate *J. Phys. D: Appl. Phys.* **40** 1059–67
- [13] Mary P, Chateauminois A and Fretigny C 2006 Contact deformation of elastic coatings in adhesive contacts with spherical probes *J. Phys. D: Appl. Phys.* **39** 3665–73
- [14] Sergici A O, Adams G G and Muftu S 2006 Adhesion in the contact of a spherical indenter with a layered elastic half-space *J. Mech. Phys. Solids* **54** 1843–61
- [15] Polonsky I A and Keer L M 2000 A fast and accurate method for numerical analysis of elastic layered contacts *J. Tribol.—Trans. ASME* **122** 30–5
- [16] Ju Y and Farris T N 1996 Spectral analysis of two dimensional contact problems *J. Tribol.—Trans. ASME* **118** 320–8
- [17] Riche I and Villechaise B 2006 Use of the FFT to determine the subsurface stresses locally in multilayered elastic solids caused by a TEHL loading *J. Tribol.—Trans. ASME* **128** 59–66
- [18] Plumet S and Dubourg M C 1998 A 3-d model for a multilayered body loaded normally and tangentially against a rigid body: application to specific coatings *J. Tribol.—Trans. ASME* **120** 668–76
- [19] Li J and Chou T W 1997 Elastic field of a thin-film/substrate system under an axisymmetric loading *Int. J. Solids Struct.* **34** 4463–78
- [20] Bentall R H and Johnson K L 1968 An elastic strip in plane rolling contact *Int. J. Mech. Sci.* **10** 637–63
- [21] Gupta P K, Walowit J A and Finkin E F 1973 Stress distribution in plane strain layered solids subjected to arbitrary boundary loading *J. Lubr. Technol.—Trans. ASME* **95** 427–33
- [22] Miller R D W 1966 Some effects of compressibility on the indentation of a thin elastic layer by a smooth rigid cylinder *Appl. Sci. Res.* **16** 405–24
- [23] Chen W T and Engel P A 1972 Impact and contact stress analysis in multilayer media *Int. J. Solids Struct.* **8** 1257–81
- [24] King R B 1987 Elastic analysis of some punch problems for a layered medium *Int. J. Solids Struct.* **23** 1657–64

- [25] Nogi T and Kato T 1997 Influence of a hard surface layer on the limit of elastic contacts: I. Analysis using a real surface model *J. Tribol.—Trans. ASME* **119** 493–500
- [26] Yang F 2003 Axisymmetric indentation of an incompressible elastic thin film *J. Phys. D: Appl. Phys.* **36** 50–5
- [27] Yoffe E H 1988 The elastic compliance of a surface film on a substrate *Phil. Mag. Lett.* **77** 69–77
- [28] Fabrikant V I 1989 *Application of Potential Theory in Mechanics: A Selection of New Results* (Dordrecht: Kluwer)
- [29] Schwarzer N 2000 Arbitrary load distribution on a layered half space *J. Tribol.—Trans. ASME* **122** 672–81
- [30] Dhaliwal R S and Rau I S 1970 The axisymmetric boussinesq problem for a thick elastic layer under a punch of arbitrary profile *Int. J. Eng. Sci.* **8** 843–56
- [31] Perriot A and Barthel E 2004 Elastic contact to a coated half-space: Effective elastic modulus and real penetration *J. Mater. Res.* **19** 600–8
- [32] Dimitriadis E K, Horkay F, Maresca J, Kachar B and Chadwick R S 2002 Determination of elastic modulus of thin layers of soft materials using the atomic force microscope *Biophys. J.* **82** 2798–810
- [33] Guizar-Sicairos M and Gutiérrez-Vega J C 2004 Computation of quasi-discrete hankel transforms of integer order for propagating optical wave fields *J. Opt. Soc. Am. A* **21** 53–8
- [34] Ku T C, Kingsley S C and Ramsey H 1965 Stresses in a thin slab with different elastic properties from that of the substrate due to distributed normal and shearing forces on the surface of the slab *Int. J. Eng. Sci.* **3** 93–107
- [35] Hills D A, Nowell D and Sackfield A 1993 *Mechanics of Elastic Contacts* (Portsmouth, NH: Heinemann)
- [36] Gacoin E, Chateauinois A and Fretigny C 2006 Measurement of the mechanical properties of thin films mechanically confined within contacts *Tribol. Lett.* **21** 245–52